

Electronic Supplementary Information (ESI)

**Bismuth chromate ($\text{Cr}_2\text{Bi}_3\text{O}_{11}$): A new bismuth-based
semiconductor with excellent photocatalytic activity**

Xinyu Gao ^{a,#}, Kelei Huang ^{a,#}, Zisheng Zhang ^b and Xiangchao Meng ^{a,*}

*^a Key Laboratory of Marine Chemistry Theory and Technology, Ministry of Education,
College of Chemistry and Chemical Engineering, Ocean University of China, Qingdao,
266100, China.*

*^b Department of Chemical and Biological Engineering, Faculty of Engineering,
University of Ottawa, Ottawa, ON, K1N6N5, Canada*

#These authors contributed equally to this work.

**Corresponding Author: mengxiangchao@ouc.edu.cn*

Contents:

1. Experimental	3
Materials.....	3
Synthesis of $\text{Cr}_2\text{Bi}_3\text{O}_{11}$	3
Characterizations	3
Photocatalytic activity tests	4
Computations.....	5
2. XPS results	6
3. TEM-EDX results	7
4. Band gap, valence band, and conduction band	8
5. PL and ESR results	9
6. Synthesis condition effect	10
7. Adsorption ability and photodegradation kinetic curves	12
8. Zeta potential	13
9. Water contact angle	14
10. Stability	15
11. Reactive free radicals capturing experiments	17
12. Photocatalytic H_2O_2 production	19
13. Summary of applications	20

1. Experimental

Materials

All materials were purchased from Sinopharm chemical reagent, except sodium chromate which was purchased from Macklin reagent, and were of analytical grade or higher purity.

Synthesis of $\text{Cr}_2\text{Bi}_3\text{O}_{11}$

$\text{Cr}_2\text{Bi}_3\text{O}_{11}$ was prepared by direct mixing. Typically, 0.750 mmol of $\text{Bi}(\text{NO}_3)_3 \cdot 5\text{H}_2\text{O}$ and 0.375 mmol of Na_2CrO_4 were dissolved in 30 mL deionized water. The mixture was magnetically stirred for 60 min at 80°C. The reaction product was filtered out while hot, washed with deionized water dried at 80°C for 12 hours, and collected for further tests. The synthesis duration, reaction temperature, pH value, molar ratio, and atmosphere were adjusted to find the optimized synthesis conditions.

Bi_2CrO_6 sample was prepared by a hydrothermal method according to our previous report (*Journal of Catalysis*, 382 (2020): 40-48.). Specifically, 0.750 mmol of $\text{Bi}(\text{NO}_3)_3 \cdot 5\text{H}_2\text{O}$ and 0.375 mmol of Na_2CrO_4 were mixed in 30 mL DDW. And the mixture was then transferred to a 50-mL Teflon-lined stainless-steel autoclave and heated to 160 °C for 20 hours. After being naturally cooled down to room temperature, the product was washed with DDW and dried at 80°C for 12 hours, and collected for further tests. Besides, Bi_2MoO_6 and Bi_2WO_6 samples were also synthesized under a similar process.

Characterizations

The crystal structure was studied using a Bruker D8 Advance X-ray diffractometer. The Fourier Transform Infrared Spectroscopy (FT-IR) was analyzed on ThermoFisher Nicolet iN10. X-ray photoelectron spectroscopy (Thermo ESCALAB XI+) was used to analyze

the surface chemical composition and the position of the valence band. Field emission scanning electron microscope (SEM, ZEISS GeminiSEM 300) was applied to study morphology. Transmission electron microscope (TEM, JEM 2100F) with energy dispersive X-ray (EDX) spectrometer was performed to observed the morphology and element content. The UV-Vis Diffuse Reflectance Spectrum (UV-Vis DRS) of the sample was characterized by the UV-Vis spectrophotometer (TU-1901). Zeta potential was detected to analyze the electrification of the sample surface. Hydrophilic contact angle with water was investigated. Oxygen vacancies and active species were characterized using electron spin paramagnetic resonance (ESR, JES FA200). The surface photovoltage (SPV) test uses the surface photovoltage test system CEL-SPS1000 from Zhongjiao Jinyuan. The Hitachi F-7100 FL Spectrophotometer was used for photoluminescence (PL) spectroscopy with an excitation wavelength of 340 nm. The elemental content was analyzed by ICP-OES (Agilent 5110).

Photocatalytic activity tests

Photocatalytic activity of the synthesized sample was evaluated regarding the degradation of the organic pollutant in water under simulated sunlight. The reactor was consisted of a 500-mL beaker with a colling jacket to maintain the temperature at 25 °C. The light source is a 300-W xenon lamp with an AM 1.5 simulated solar filter. In each test, 100 mL of organic pollutant solution with an initial concentration of 5 mg/L was added into the reactor, and 1 g/L of catalyst was dispersed in the solution. After stirring for 30 min in the dark to obtain an adsorption-desorption equilibrium, the photocatalytic process was started by switching on the lamp, and lasted for 30 min (or 1 hour). In each test, 1.5 mL of

suspension was taken from the reactor, and the supernatant was analyzed by UV-Vis spectrophotometer (TU-1901) after centrifugation. The change of total organic carbon (TOC) in the degradation of phenol was analyzed with a total organic carbon detector (ELEMENTAR, vario TOC).

The photocatalytic oxidation of water to evolve O₂ was carried out in a photoreactor with a fixed temperature of 25°C, which is connected to a glass gas system (Labsolar-6A, PerfetLight). With Fe(NO₃)₃ as a sacrificial agent, 100 mg of the photocatalyst was suspended in 100 mL of Fe(NO₃)₃ aqueous solution (10 mmol·L⁻¹). Then, a 300 W xenon lamp was applied to thoroughly degas and irradiate the suspension. The gas discharged at regular intervals was analyzed with an on-line gas chromatograph (GC-7900/Techcomp, TCD detector, Ar carrier).

Computations

Density functional theory (DFT) simulations were performed using the Vienna *ab initio* Simulation Program (VASP), and Vesta was used for the plot.

2. XPS results

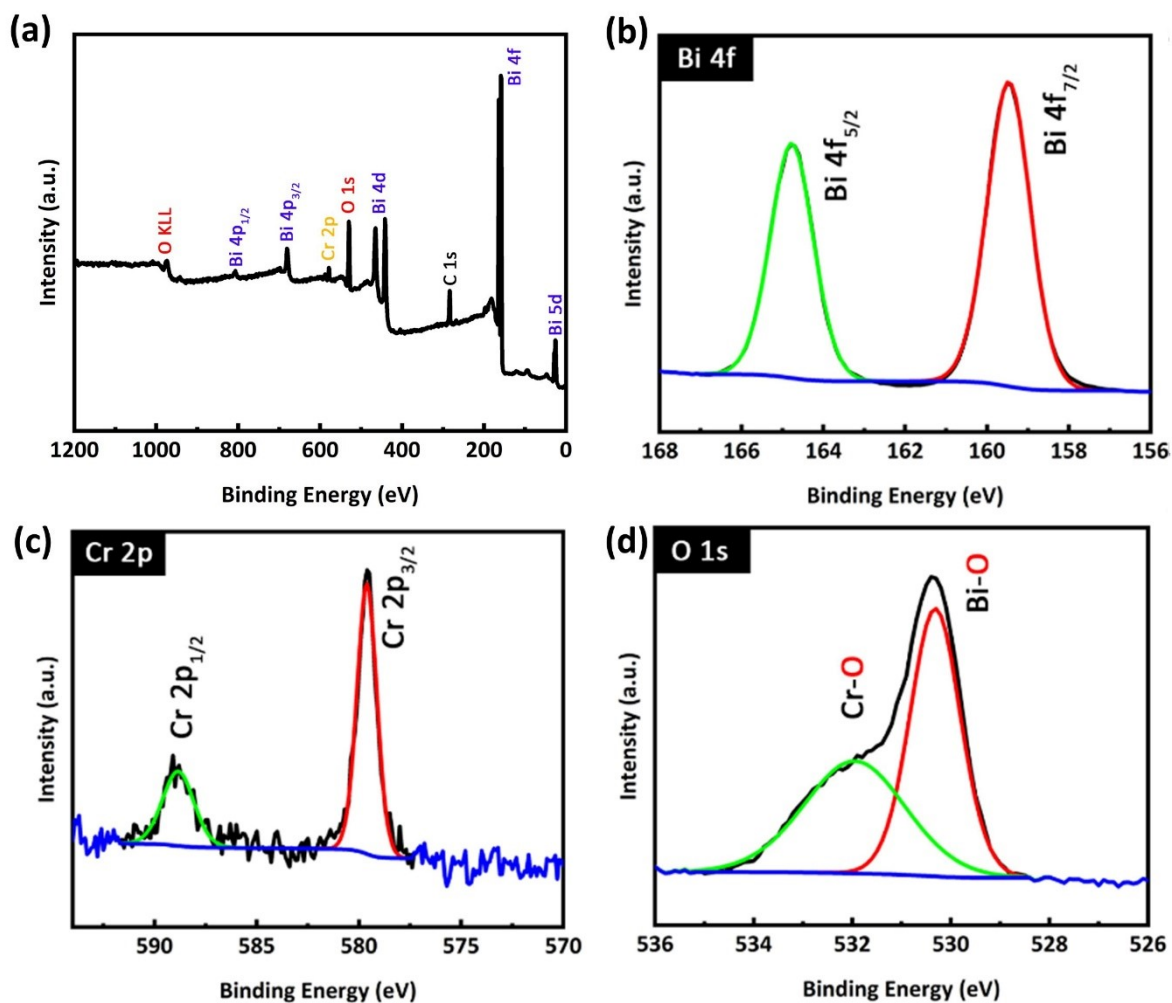


Fig. S1. XPS spectra of $\text{Cr}_2\text{Bi}_3\text{O}_{11}$: (a) Survey, (b) Bi 4f, (c) Cr 2P, and (d) O 1s.

3. TEM-EDX results

From the TEM-EDX results, the atomic ratio of Cr/Bi/O was determined about 11.98/17.50/70.53 (Table S1), which was close to the stoichiometry ratio 2/3/11 of $\text{Cr}_2\text{Bi}_3\text{O}_{11}$ compound.

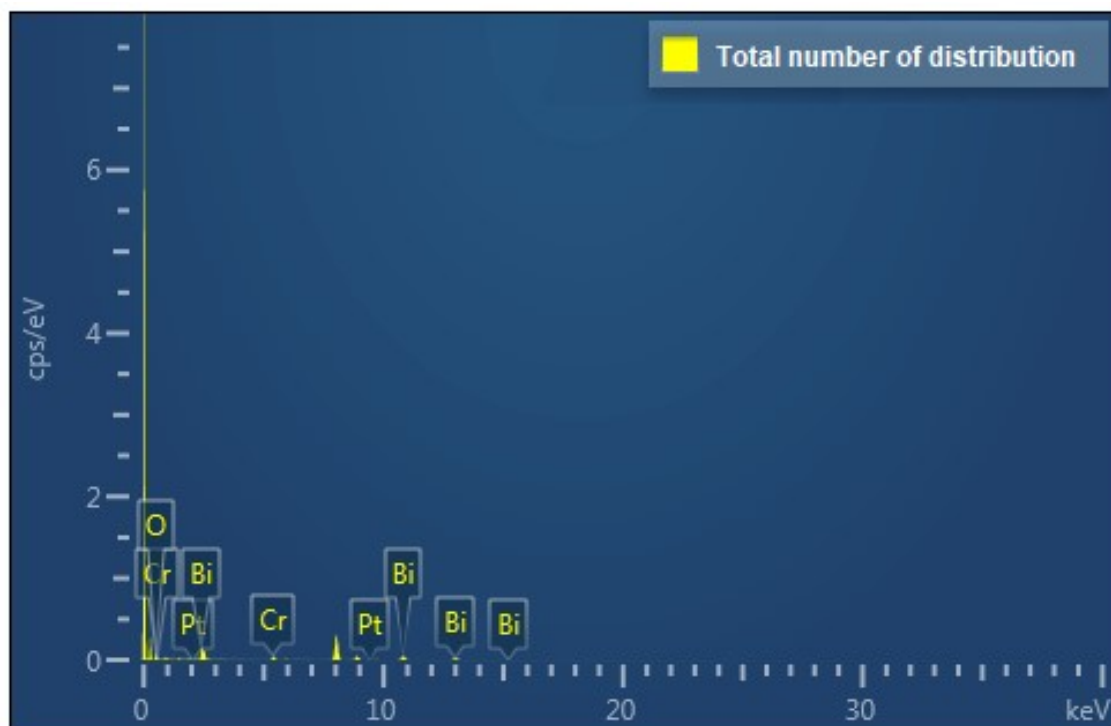


Fig. S2 EDX total number of distributions.

Table S1 Atomic distribution statistics of $\text{Cr}_3\text{Bi}_2\text{O}_{11}$.

Element	k factor	wt.%	wt.% Sigma	Atomic percentage/%
O	1.998	20.87	0.92	70.53
Cr	1.123	11.52	0.55	11.98
Bi	2.629	67.61	1.05	17.50
Total		100.00		100.00

4. Band gap, valence band, and conduction band

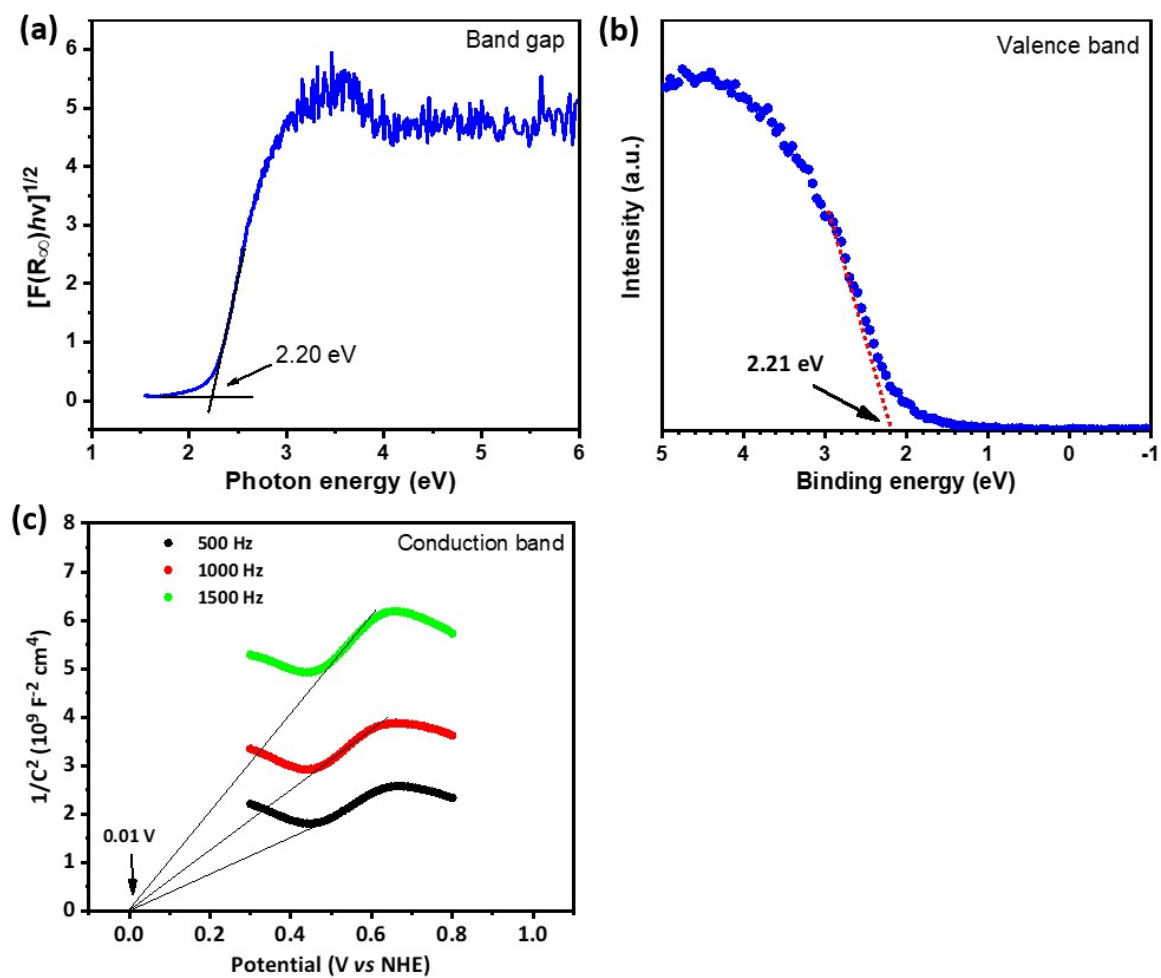


Fig. S3. (a) $Cr_2Bi_3O_{11}$ plots of transformed Kubelka-Munk function versus photon energy; (b)

XPS-VB spectra of $Cr_2Bi_3O_{11}$; (c) Mott-Schottky plots of $Cr_2Bi_3O_{11}$.

5. PL and ESR results

As shown in Fig. S4a, the Bi_2CrO_6 showed the high PL intensity due to its high recombination of photogenerated electrons and holes. Besides, the ESR measurement was conducted to study the structural defects of $\text{Cr}_2\text{Bi}_3\text{O}_{11}$ and Bi_2CrO_6 (Fig. S4b). Both exhibited an obvious peak at $g = 2.001$, which was attributed to the oxygen vacancies (J. Hazard. Mater. 403 (2021): 123661; Sol. RRL 4 (2020): 2000037; Appl. Catal. B-Environ. 231 (2018): 357-367). Higher peak on Bi_2CrO_6 sample suggested the higher concentration of oxygen vacancies, which might become the trapping center of photogenerated charges leading to the high recombination rate.

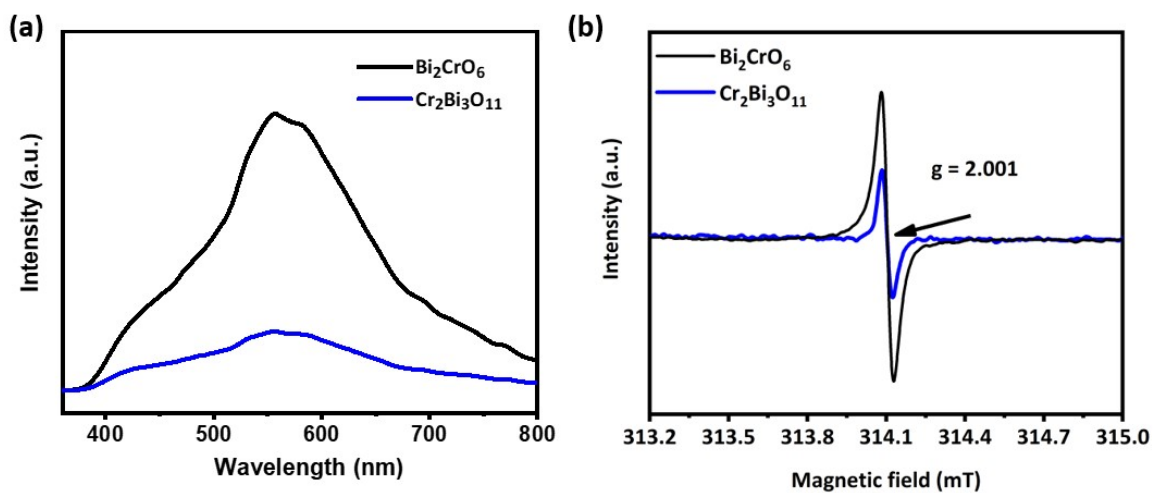


Fig. S4. (a) PL results and (b) ESR results of $\text{Cr}_2\text{Bi}_3\text{O}_{11}$ and Bi_2CrO_6 .

6. Synthesis condition effect

The controlled synthesis of bismuth chromate was studied. Through the degradation of the dye represented by 5 ppm RhB under the AM 1.5 simulated sunlight, the regular pattern between the synthesis conditions and activities of the samples was explored. First, at room temperature (about 25 °C), a series of $\text{Cr}_2\text{Bi}_3\text{O}_{11}$ samples with different reaction times were synthesized. As shown in Fig. S5a, the sample prepared by 1 h synthesis time) showed the highest degradation efficiency for RhB. Synthesis time less than 1 h was not enough for crystal growth. And Over 1h, $\text{Cr}_2\text{Bi}_3\text{O}_{11}$ may have a slow side reaction with excess reactants in the synthesis system. After determining the optimal reaction time of 1h, a series of samples at multiple reaction temperatures were synthesized (Fig. S5b). The optimal temperature was 80 °C. Higher temperature may be more conducive to the growth of $\text{Cr}_2\text{Bi}_3\text{O}_{11}$ crystals, so the catalyst synthesized under higher temperature conditions has better catalytic efficiency. Under the condition of 90°C, water is close to the boiling point and the temperature fluctuates greatly, which may affect the crystal growth. The ratio of bismuth to chromium in the reactant was also investigated (Fig. S5c). From the results, the sample prepared when the ratio of bismuth to chromium is 2:1 has the highest activity. It means that excessive amounts of $\text{Bi}(\text{NO}_3)_3 \cdot 5\text{H}_2\text{O}$ or Na_2CrO_4 will affect the normal synthesis and crystal growth of $\text{Cr}_2\text{Bi}_3\text{O}_{11}$. The sample of $\text{Cr}_2\text{Bi}_3\text{O}_{11}$ showed the highest catalytic efficiency when synthesized in deionized water (pH 6.56). The efficiency of catalysts synthesized in an acid or alkaline environment was slightly decreased. H^+ and OH^- may be adsorbed on some sites of $\text{Cr}_2\text{Bi}_3\text{O}_{11}$ and hinder its normal growth (Fig. S5d). Furthermore, the nitrogen aeration, oxygen aeration, and air atmosphere of the synthesis

system were explored (Fig. S5e). The best photocatalytic activity was observed over the $\text{Cr}_2\text{Bi}_3\text{O}_{11}$ synthesized in air. Sample synthesized under the O_2 atmosphere showed lower efficiency, which might mean that a large amount of oxygen was not conducive to the synthesis of $\text{Cr}_2\text{Bi}_3\text{O}_{11}$.

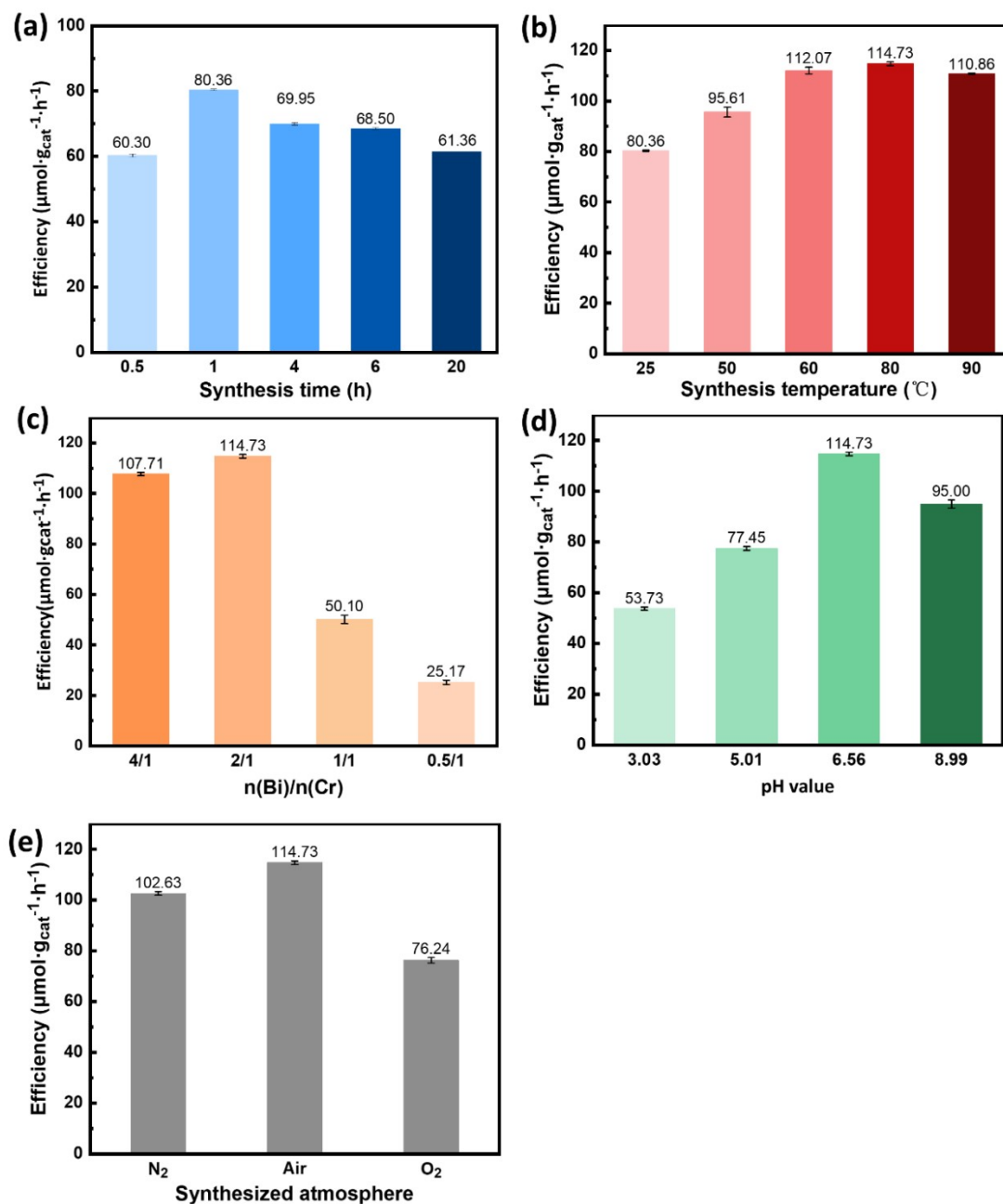


Fig. S5. Photodegradation RhB dye (AM 1.5 simulated sunlight, 5 ppm RhB, 30 min) over $\text{Cr}_2\text{Bi}_3\text{O}_{11}$ synthesized under different condition: (a) time, (b) temperature, (c) n(Bi)/n(Cr) ratio, (d) pH value, and (e) atmosphere.

7. Adsorption ability and photodegradation kinetic curves

Fig. S6a exhibited the adsorption ability for dyes (RhB, MB, and MO) and phenol over $\text{Cr}_2\text{Bi}_3\text{O}_{11}$. After 30 min dark adsorption, the equilibrium of adsorption and desorption was acquired. The adsorption amount of phenol was lowest and the adsorption amount of RhB was the highest. Besides, the kinetics of pollutants photocatalytic degradation were investigated by the pseudo-first-order model: $-\ln(C/C_0) = kt$, and the results were shown in Fig. S6b and S6c.

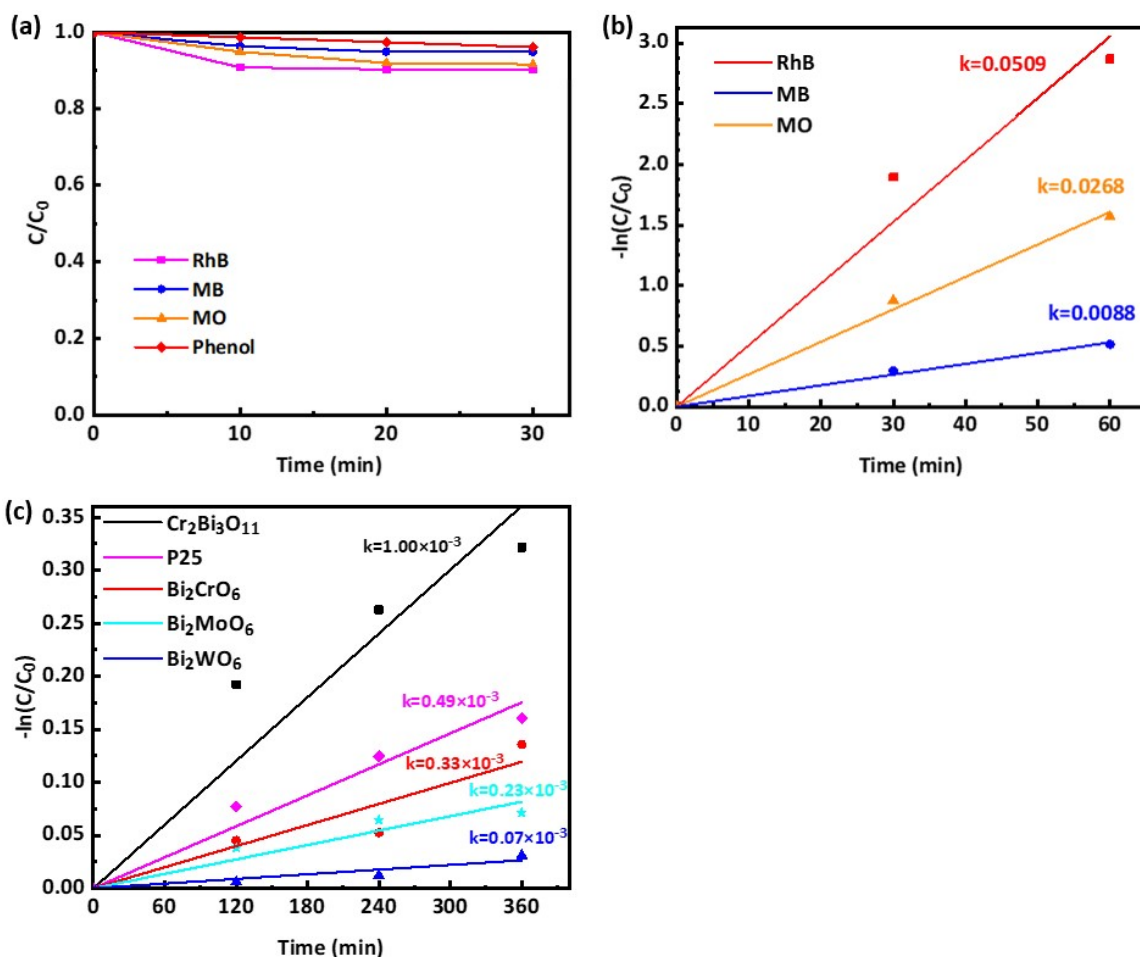


Fig. S6. (a) Adsorption ability for dyes (RhB, MB, and MO) and phenol over $\text{Cr}_2\text{Bi}_3\text{O}_{11}$; (b) Fig. 4b corresponding kinetic curves of photodegradation dyes over $\text{Cr}_2\text{Bi}_3\text{O}_{11}$; (c) Fig. 4c corresponding kinetic curves of photodegradation phenol over $\text{Cr}_2\text{Bi}_3\text{O}_{11}$, P25, and Bi_2MO_6 ($M = \text{Cr, Mo, or W}$).

8. Zeta potential

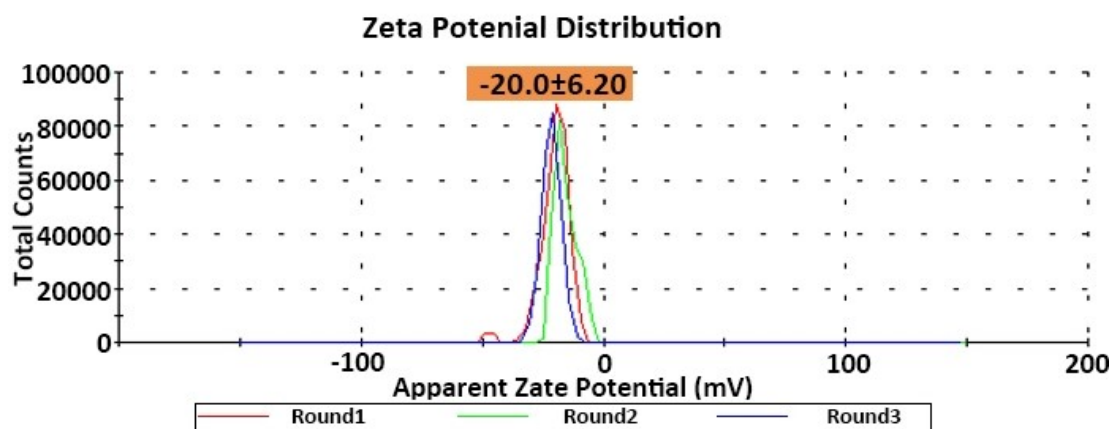


Fig. S7. Zeta potential of $\text{Cr}_2\text{Bi}_3\text{O}_{11}$.

9. Water contact angle

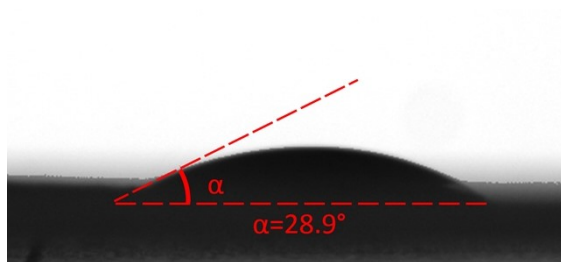


Fig. S8. Water contact angle of $\text{Cr}_2\text{Bi}_3\text{O}_{11}$.

10. Stability

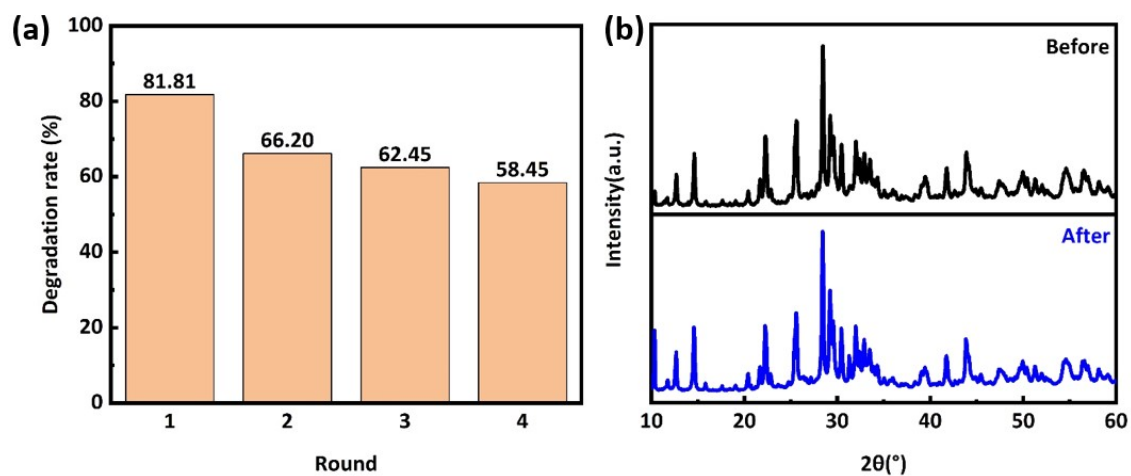


Fig. S9. (a) Degradation cycling test (AM 1.5 Simulated sunlight, 5 ppm RhB, 60 min). (b) XRD patterns of $\text{Cr}_2\text{Bi}_3\text{O}_{11}$ before and after cycling test.

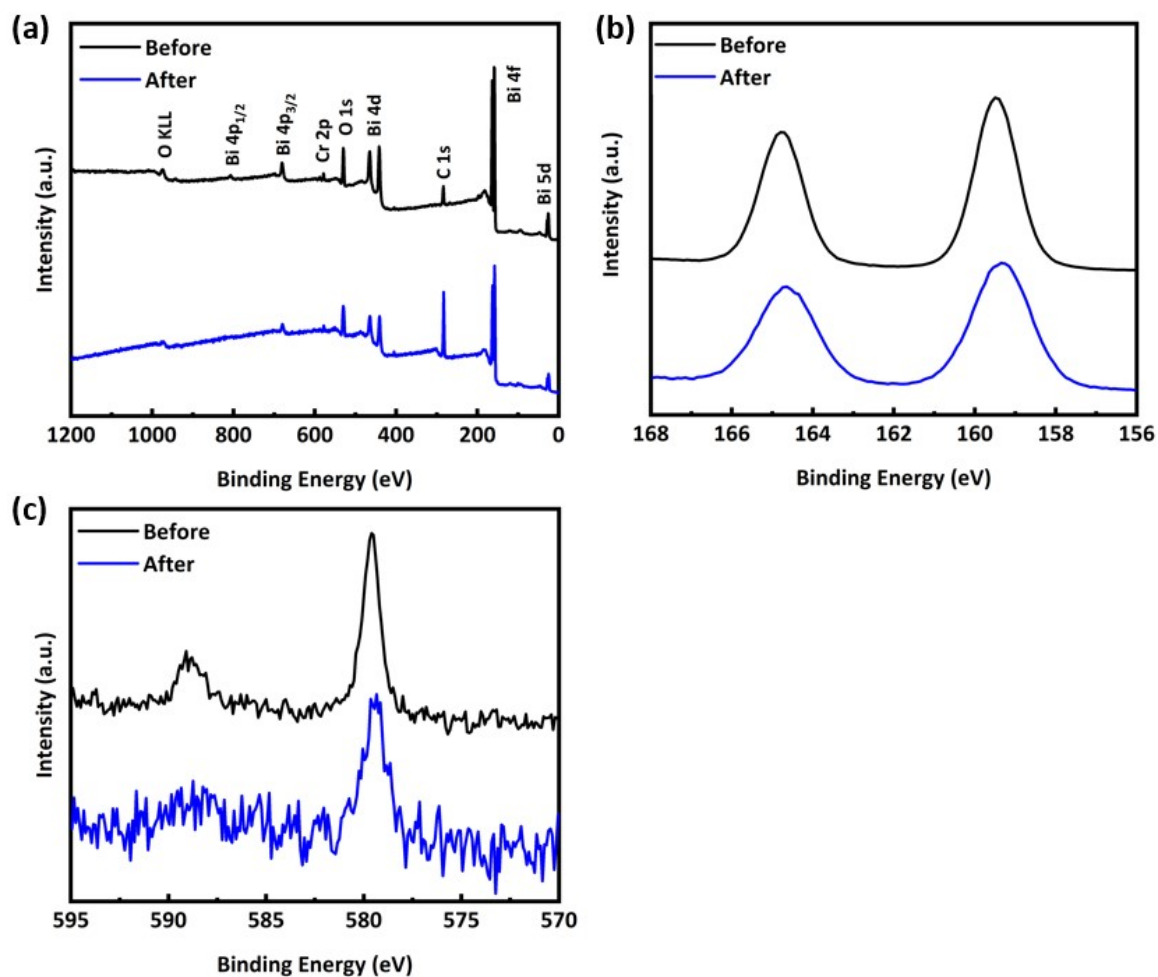


Fig. S10. XPS spectra of (a) survey, (b) Bi 4f and (c) Cr 2p before and after the reaction (AM 1.5 Simulated sunlight, 5 ppm RhB, 60 min)

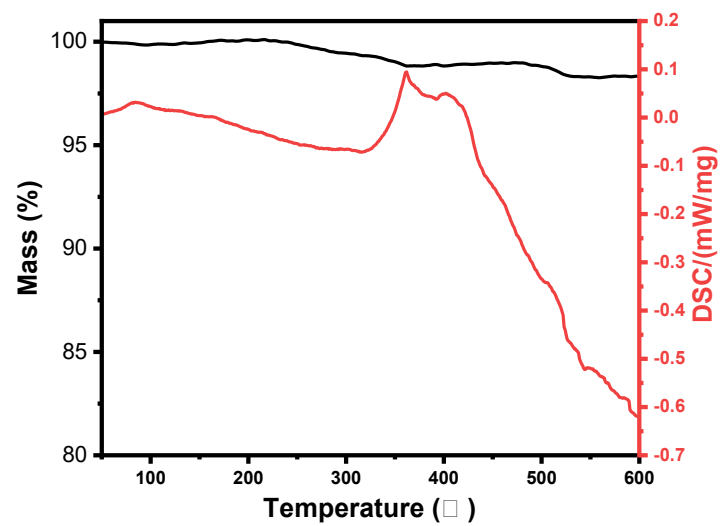


Fig. S11. Thermogravimetric (TG) curve of $\text{Cr}_2\text{Bi}_3\text{O}_{11}$ under air atmosphere.

11. Reactive free radicals capturing experiments

Fig. S12a and S12b showed the main active species during organic pollutant were $\cdot\text{O}_2^-$ and $\cdot\text{OH}$. To further confirm the production of $\cdot\text{O}_2^-$ and $\cdot\text{OH}$ active species by $\text{Cr}_2\text{Bi}_3\text{O}_{11}$, the electron spin resonance (ESR) was carried out by using 5, 5-dimethyl-1-pyrroline-N-oxide (DMPO) as trapping agent under light irradiation. As shown in Fig. S12c and S12d, no ESR signal could be observed under dark. After light irradiation, four characteristic peaks with an intensity ratio of 1:1:1:1 were observed (Fig. S12c), which was assigned to the DMPO- $\cdot\text{O}_2^-$ adducts. Besides, four characteristic peaks with an intensity ratio of 1:2:2:1 attributed to DMPO- $\cdot\text{OH}$ adducts were observed (Fig. S12d).

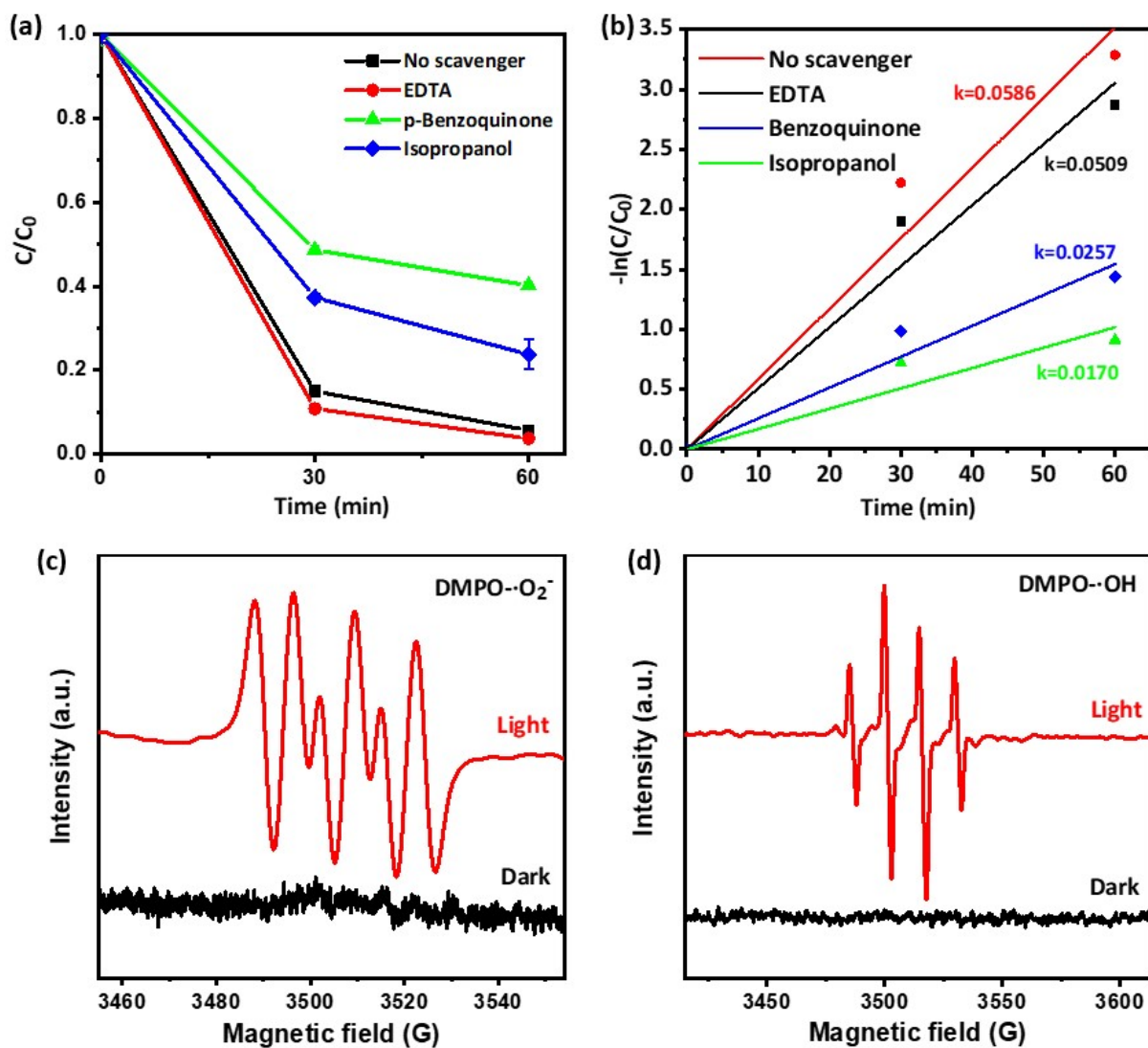


Fig. S12. (a) Degradation RhB over $Cr_2Bi_3O_{11}$ (AM 1.5 simulated sunlight, 5 ppm RhB) with adding three trapping agents (1 mmol/L): ethylenediamine tetraacetic acid (EDTA) for holes, isopropanol for $\cdot OH$, and p-benzoquinone for $\cdot O_2^-$, and (b) corresponding kinetic curves. ESR spectra of radical species trapped by 5, 5-dimethyl-1-pyrroline-N-oxide (DMPO) after 10 min light irradiation with (c) methanol and (d) aqueous dispersion.

12. Photocatalytic H₂O₂ production

The experiment of photocatalytic production of hydrogen peroxide (H₂O₂) was carried out at 25°C. Suspended 0.1 g of catalyst in an open system of 95 mL of distilled water and 5 mL of ethanol, and stir for 30 min in the dark to make the system reach equilibrium. Then, the system was irradiated with visible light (> 400 nm) for 3 h, and 1 mL suspension was taken out every 30 min, mixed with 2 mL 0.1M KI solution and 1 mL of ammonium molybdate solution (0.01 M). The absorbance was detected by UV-Vis spectrophotometer to determine the concentration of H₂O₂.

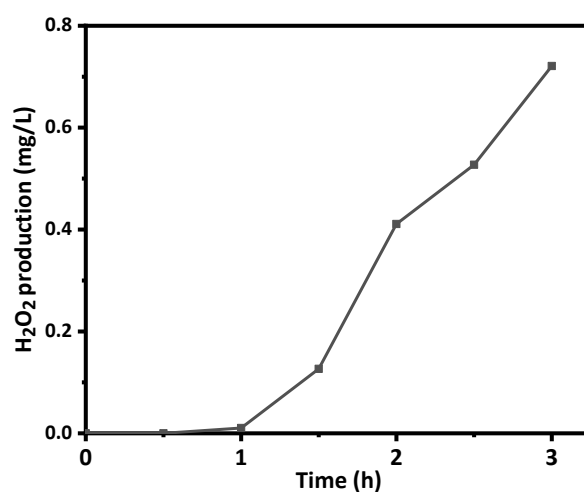


Fig. S13. Photocatalytic H₂O₂ production activity over Cr₂Bi₃O₁₁.

13. Summary of applications

This photocatalyst showed good activity in the photooxidative degradation of dyes and phenol, and exhibited the activity of OER and H₂O₂ production. But it did not show activity in reactions such as HER, NRR, CO₂RR, and 4-nitroaniline reduction.

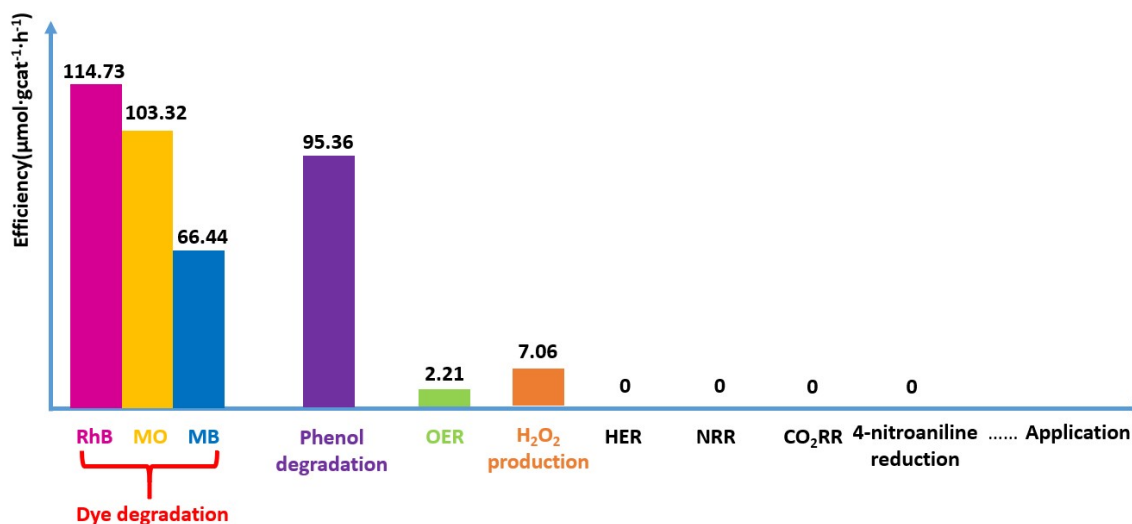


Fig. S14. Photocatalytic activities of different applications that have been tested over Cr₂Bi₃O₁₁.